

# Surface Modification and Preparation of Nanofiltration Membrane from Polyethersulfone/Polyimide Blend—Use of a New Material (Polyethyleneglycol-Triazine)

Yaghoub Mansourpanah,<sup>1</sup> Sayed Siavash Madaeni,<sup>1</sup> Mohsen Adeli,<sup>2</sup> Ahmad Rahimpour,<sup>1</sup> Arman Farhadian<sup>1</sup>

<sup>1</sup>Department of Chemical Engineering, Membrane Research Center, Razi University, Tagh Bostan, Kermanshah 67149, Iran

<sup>2</sup>Department of Chemistry, Lorestan University, Khorramabad, Iran

Received 12 February 2008; accepted 24 November 2008

DOI 10.1002/app.29821

Published online 24 February 2009 in Wiley InterScience (www.interscience.wiley.com).

**ABSTRACT:** Blends of polyethersulfone/polyimide (PES/PI) were prepared by dissolving in dimethylformamide/dioxane (DMF/DO) to manufacture nanofiltration membranes by using polyvinylpyrrolidone (PVP) as a pore former. The membrane modification was carried out by adding ethylenediamine (EDA) to open the imide group ring of PI and by using polyethyleneglycol (PEG)-triazine, as a new modifier material, that was produced in the laboratory. This modification involves the formation of a covalence -C-N- bound between PEG-triazine and amine groups (according to addition-elimination reactions) at different temperatures. After functionalizing the membranes, diethanolamine (DA) was utilized as a hydrophilic modifier to change the membranes properties. SEM, AFM, FTIR-ATR, EDS (X-ray analysis) and contact angle tests

were carried out to characterize modified membranes. The hydrophilicity of PES/PI membranes was improved by modification. An increase in pure water flux (up to 195 kg/m<sup>2</sup> h) and a decline in NaCl rejection (from 25 to 16%) are largely influenced by diminishing the PES/PI ratio in L<sub>1</sub>-L<sub>5</sub> membranes (Category 1). In L<sub>6</sub>, L<sub>7</sub>, and L<sub>8</sub> membranes (Category 2), by introducing PEG-triazine into the membrane recipe, salt rejection increased from 75 to 80%. Addition of DA further enhances the salt rejection up to 93%. Fluxes were approximately similar for membranes in Category 2. © 2009 Wiley Periodicals, Inc. *J Appl Polym Sci* 112: 2888–2895, 2009

**Key words:** nanofiltration surface modification; PES/PI blend; hydrophilicity variation; PEG-triazine

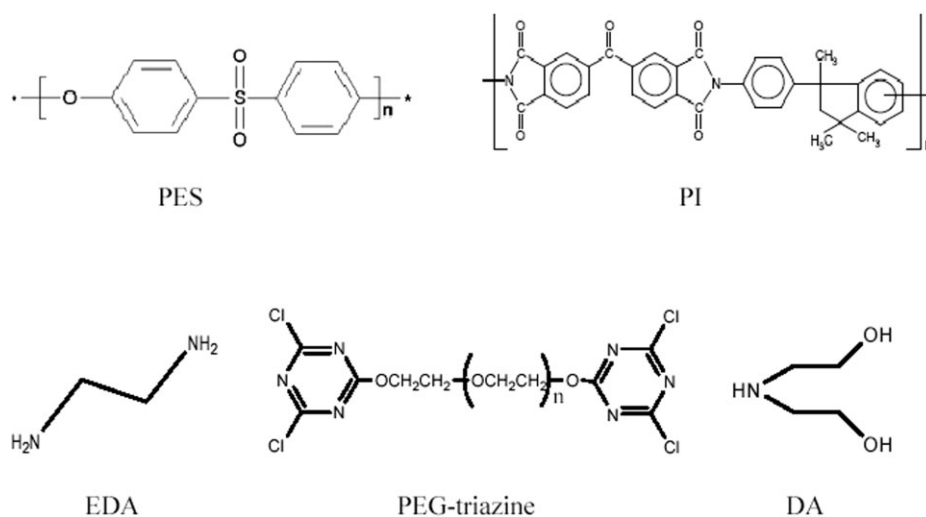
## INTRODUCTION

In the recent years, nanofiltration (NF) technology has been used for concentration, purification, and fractionation of various products in diverse fields.<sup>1–8</sup> Nanofiltration membranes provide specific advantages over conventional reverse osmosis membranes. NF normally provides a higher water flux and operates at lower pressures, which reduces energy consumption. Most of the commercial nanofiltration membranes are made from hydrophobic polymers like polysulfone, polyethersulfone, polyvinylidene-fluoride, and polyimide because of their excellent chemical resistance and thermal and mechanical properties. But, hydrophobic membranes are easily susceptible to fouling and severe decline in permeate flux with operation time.<sup>9</sup> It has been generally acknowledged that membranes with a hydrophilic

surface are better for filtration.<sup>10</sup> Thus, surface modification of membranes is an attractive approach to changing the surface properties. Several techniques have been employed to impart surface hydrophilicity to conventional hydrophobic membranes. These techniques include (1) radiation and photochemical grafting of hydrophilic polymers,<sup>11</sup> (2) glow discharge low temperature plasma treatments,<sup>12</sup> (3) covalent attachment of hydrophilic polymers and functional monomers,<sup>13</sup> and (4) coating of a thin layer of a hydrophilic polymer on membrane surface by physical absorption.<sup>14</sup> Polyethersulfone and polyimide possess excellent mechanical and film-forming properties and also a high thermal stability, which make them ideal materials for membrane manufacturing. However, these polymers are hydrophobic. Preparation of membranes from polymer blend is rapidly expanding. Polymer blends belong to the heterogeneous category.<sup>15</sup> Liang et al.<sup>16</sup> showed that the blend of polyethersulfone and polyimide is miscible in a wide range of compositions. Ekiner prepared polyethersulfone-polyimide membranes for gas separation.<sup>17</sup> Kapantaidakis and Koops studied the formation and gas permeation properties of

Correspondence to: S. S. Madaeni (smadaeni@yahoo.com).

Contract grant sponsors: New Technologies Centre, Ministry of Industry of Iran.



**Scheme 1** Chemical structure of PES, PI, EDA, PEG-triazine, and DA.

hollow fiber membranes based on PES/PI blends.<sup>18</sup> The fibers had a porous skin layer, a loose sub layer, and a high permeation values. Powell et al.<sup>19</sup> used diamines to crosslink polyimide via reaction with carbonyl groups. Polyimide is a convenient polymer for membrane preparation and modification, due to excellent physical properties and tunable chemical composition by utilizing different molecular structures composed of dianhydride and diamine monomers.<sup>20</sup>

In this research, flat sheet membranes were prepared from a PES/PI blend, with PES as matrix and PI as a polymer that may be functionalized with ethylenediamine (EDA) and PEG-triazine. This provides a membrane with coupling or reactive sites.

## EXPERIMENTAL

### Material and apparatus

Polyethersulfone (PES Ultrason E6020P with  $M_w = 58,000$  g/mol) was supplied by BASF Company (Germany). Polyvinylpyrrolidone (PVP) with 25,000 g/mol molecular weight, *N,N*-dimethylformamide (DMF), 1,4-dioxane (DO), ethanol, methanol, benzylamine, diethanolamine (DA), and ethylenediamine (EDA) from Merck were used. Poly (ethylene glycol) 1000, cyanuric chloride, sodium hydroxide, dichloromethane, and diethyl ether were purchased from Merck and used for preparation of PEG-triazine. Polyimide (PI) was purchased from Alfa Aser Company (Germany). The steric structure of PES, PI, EDA, PEG-triazine, and DA is depicted in Scheme 1. The rejection of NaCl (from Merck) was investigated by measuring the amount of ions in the permeate by using Atomic Adsorption (Shimadzu Model AA-670). Distilled water was used throughout the study.

### Preparation of PEG-triazine

A solution of poly (ethylene glycol) (4 g,  $4 \times 10^{-3}$  mol) and sodium hydroxide (0.32 g,  $8 \times 10^{-3}$  mol) in 10 mL of water was added to a solution of cyanuric chloride (3.69 g,  $2 \times 10^{-2}$  mol) in 50 mL dichloromethane. The mixture was stirred at 0°C for 1 h, then it was stirred at the room temperature for 1 h, and finally was refluxed for an additional 6 h. The mixture was cooled and filtered and the solvent was evaporated. The crude product was dissolved in 10 mL of dichloromethane and was precipitated in diethyl ether at 0°C several times. The purified product was obtained as a white solid (5.1 g,  $4 \times 10^{-3}$  mol, 100%). IR:  $2877\text{ cm}^{-1}$  was assigned to aliphatic hydrogens (C–H), 1755, 1714, and  $1669\text{ cm}^{-1}$  were assigned to C=N bounds in triazine ring,  $1111\text{ cm}^{-1}$  was assigned to C–O in Poly(ethylene glycol) backbone.  $^1\text{H}$  NMR (DMSO- $d_6$ ): 3.48–3.54 was assigned to H atoms in the final  $\text{CH}_2$  group in vicinity of triazine ring ( $-\text{CH}_2\text{O-triazine}$ ), 3.63–3.68 was assigned to H atoms in PEG.  $^{13}\text{C}$  NMR (DMSO- $d_6$ ): 69 was assigned to C atoms in PEG backbone, 71 was assigned to C atoms of the final  $\text{CH}_2$  group in vicinity of triazine ring ( $-\text{CH}_2\text{O-triazine}$ ), 150 was assigned to C atoms in triazine ring. The details and more explanations may be found in the published literature from the current authors.<sup>21,22</sup>

### Preparation of membranes

Different blend solutions of PES/PI with total concentration of 18 wt % (16/2, 14/4, and 12/6 wt %) was prepared by dissolving in DMF/DO (50/50 wt %) and by using 2 wt % polyvinylpyrrolidone as a pore former. The stirring was carried out at 200 rpm for 5 h at 50°C. After formation of a homogeneous solution, the dope solution was hold at ambient

**TABLE I**  
**Composition of Membranes**

Membrane	PES/PI blend composition (wt %)	PVP	Composition of modification solution (wt %)		
			EDA	PEG-Triazine	DA
Category 1					
L <sub>1</sub>	16/2	2	–	–	–
L <sub>2</sub>	14/4	2	–	–	–
L <sub>3</sub>	12/6	2	–	–	–
L <sub>4</sub>	12/6	2	5	0.5	1
L <sub>5</sub> <sup>a</sup>	12/6	2	5	0.5	5
L <sub>6</sub>	19/2	2	–	–	–
Category 2					
L <sub>7</sub>	19/2	2	5	0.5	–
L <sub>8</sub> <sup>b</sup>	19/2	2	5	0.5	5

<sup>a</sup> Total PES/PI concentration for Category 1 = 18 wt %.

<sup>b</sup> Total PES/PI concentration for Category 2 = 21 wt %.

temperature for around 3.5 h to remove the air bubbles. Afterward, the dope solution was cast on a smooth glass plate at 250 μm height using a film applicator at the room temperature without evaporation. All experiments were conducted at the room temperature. The films were directly immersed in a coagulation bath (distilled water 90 v% and ethanol 10 v%) at the room temperature. After primarily phase separation, the membrane was formed. The prepared membrane was stored in the coagulation bath for 20 h for completion of phase separation. The membrane was placed between two sheets of filter papers for 24 h at the room temperature to dry.

### Modification and post-treatment of membranes

The PES/PI (12/6 wt %) was selected as the base dope solution for membrane preparation. The prepared and dried membranes were immersed in methanol comprising 5 wt % EDA. After 3 h the membranes were demounted, carefully washed with pure methanol to remove unadsorbed EDA, and dried for 24 h. The membrane color was converted from yellow to white. Subsequently, the membranes were immersed for 3 h in a 5 wt % PEG-triazine aqueous solution. To change the hydrophilicity of the membranes, aqueous solutions containing 1 and 5 wt % DA were employed. DA was dissolved in distilled water. The obtained membranes were immersed in the solution for 3 h at 70°C in a sealed vessel. Finally, three membranes with 19/2 wt % of PES/PI (total concentration of 21 wt %) were prepared and modified according to the above-mentioned method. All membranes were classified into two categories. The first category included L<sub>1</sub> to L<sub>5</sub> and the second class comprised L<sub>6</sub> to L<sub>8</sub>. The compositions of all membranes are listed in Table I. Briefly, the occurred reaction is nucleophilic and electro-

philic addition. EDA is a nucleophilic reagent that attacks carbonyl groups (electrophilic reagent) and opens the imide's ring of PI. One of the chlorine atoms of triazine ring is substituted by another amine group of DEA. This reaction occurred at the room temperature. For removal of other chlorine atoms from the triazine ring by DA, a temperature around 70°C is required. The second chlorine atom from the triazine ring can be substituted by nitrogen atoms of DA as a result of nucleophilic reaction. Another ring of PEG-Triazine can react with adjacent EDA-modified imide ring or with another group far away.

## CHARACTERIZATION METHODS

### Permeation test

The performances of the prepared membranes were characterized using a cross-flow batch system. The details of the experimental set up are described elsewhere.<sup>23</sup> All filtration experiments were carried out in a cross-flow cell with the membrane surface area of 22 cm<sup>2</sup>. One coupon was tested for each experiment. The retentate was circulated by a pump. To measure the membrane capability for ion rejection, salt solutions were employed as the feed. The amount of ions in the feed and the permeate were analyzed by using Atomic Adsorption (Shimadzu Model AA-670). The flux of each membrane was determined in 30 min for the NaCl solution with a transmembrane pressure around 0.5 MPa. The experiments were carried out at 25°C. Cross-flow velocity was selected around 1 m/s for all trials. Each membrane was precompressed with pure water at 0.5 MPa for 1 h at 1 m/s velocity before experiments. The adsorbed reagents, if it happened, were removed from the surface as a result of this process. The permeation rate and the salt rejection were determined for all prepared membranes by using a 2000 mg/L NaCl solution. The collected permeate was measured by a digital balance with an accuracy of 0.001 g. To minimize the salt concentration error in the permeate, the experiments were carried out three times. The rejection may be described by the following equation:

$$R\% = \left[ 1 - \frac{C_p}{C_f} \right] \times 100 \quad (1)$$

where  $C_p$  is ion concentration in the permeate and  $C_f$  is ion concentration in the feed.

### FTIR-ATR measurements

Chemical changes in the membranes before and after crosslinking were monitored by using an Equinox 55 Bruker FT-IR spectrometer with a total reflection



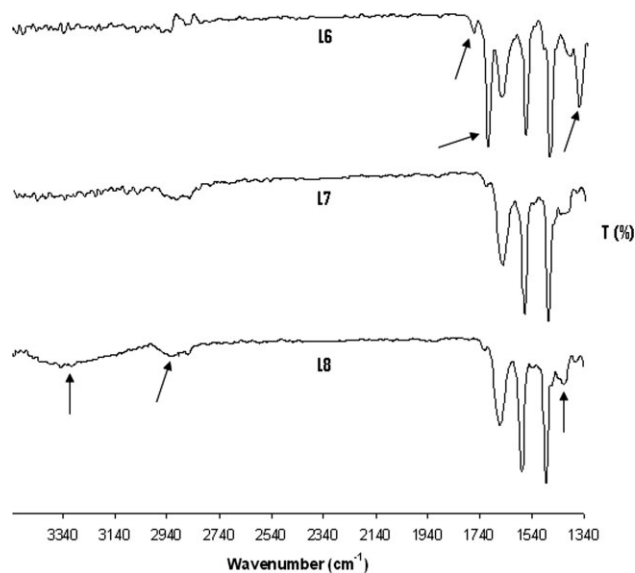


**Figure 1** The comparison FTIR-ATR spectra of  $L_6$ ,  $L_7$ , and  $L_8$  membranes.

attachment (ATR). Thirty-two scans were measured during the IR study for each sample. The resolution of apparatus was  $4\text{ cm}^{-1}$ .

#### Microscopic (SEM, AFM and EDS) studies

SEM and AFM microscopes were employed for investigation of membrane morphology, surface property, and pore size. SEM apparatus (Philips) was employed to obtain images of the membrane cross sections. Membranes were snapped in liquid nitrogen to break. The samples were coated with gold and viewed at 25 kV. The AFM apparatus was DualScope™ scanning probe-optical microscope (DME model C-21, Denmark). Small squares of the prepared membranes ( $\sim 1\text{ cm}^2$ ) were cut and glued on a glass substrate. The membrane surfaces were analyzed in a scan size of  $500 \times 500\text{ nm}$ . The ele-

mental analysis was carried out by an EDS (Energy Disperse spectroscopy) device (CamScan Model MV 2300) that was attached to SEM.

#### Contact angle measurements

The static contact angles were measured with a contact angle measuring instrument (G10, KRUSS, Germany). Contact angle measurements were carried out 10 days after the formation of membranes. Deionized water was used as the probe liquid in all measurements and the contact angles between water and the membrane surface were measured for the evaluation of the membrane hydrophilicity. To minimize the experimental error, the contact angle was measured at five random locations for each sample and the average [along with the standard deviation (S)] was reported.

## RESULTS AND DISCUSSION

#### FTIR-ATR spectra

To obtain the quantitative information about the modified membranes, FTIR-ATR standard curves of  $L_6$ ,  $L_7$ , and  $L_8$  membranes were plotted. Figure 1 presents the FTIR spectra for the unmodified membrane ( $L_6$ ), and modified membranes with PEG-triazine ( $L_7$ ) and with PEG-triazine and DA ( $L_8$ ). See Table I for membrane details.

Typical polyimide bands at  $1780\text{ (C=O)}$ ,  $1720\text{ (C=O)}$ , and  $1365\text{ cm}^{-1}\text{ (C-N)}$  and amide bands at  $1660\text{ (C=O)}$  and  $1570\text{ (C-N)}$  were identified to track changes to the polymer structure.

In Figure 1 the peaks at  $1723$ ,  $1775$ , and  $1370\text{ cm}^{-1}$  were assigned to the stretching vibration of  $\text{C=O}$  and  $\text{C-N}$  groups of polyimide, respectively. These peaks have been hidden in other membranes and

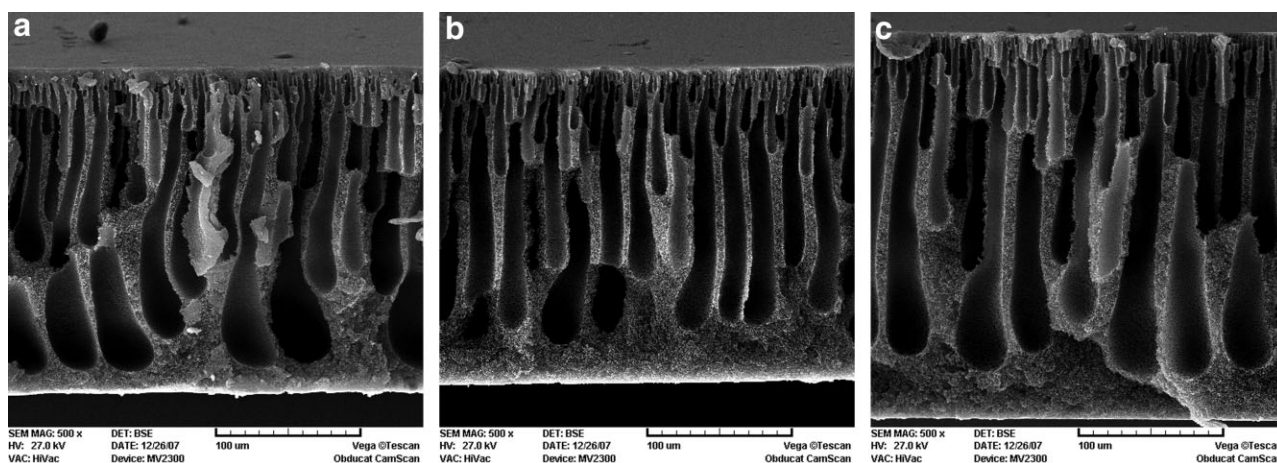


**Figure 2** Cross-sectional SEM of membrane morphology: (a)  $L_1$ , (b)  $L_2$ , and (c)  $L_3$ .

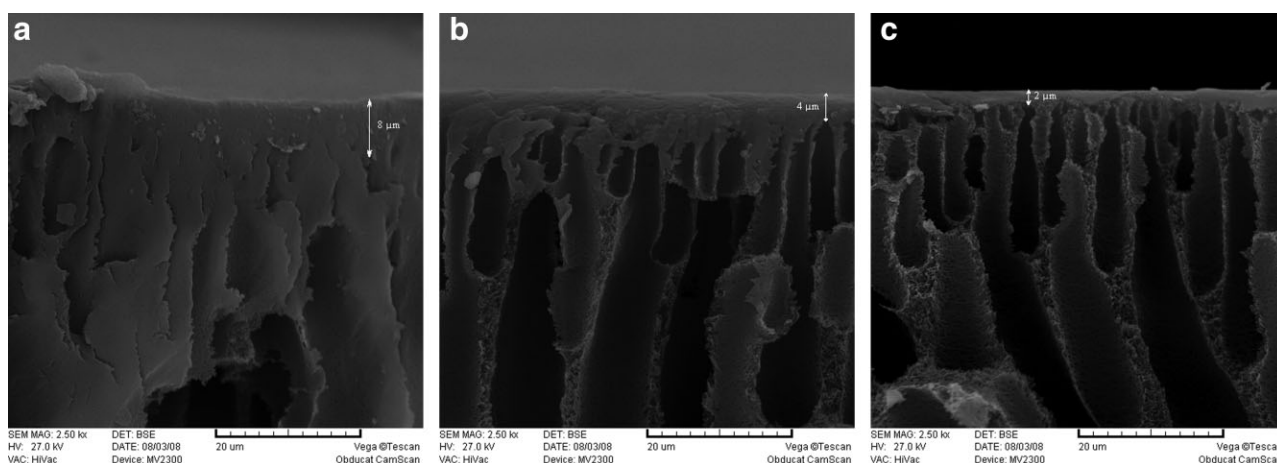


**Figure 3** Effect of PES/PI ratio on skin layer thickness: (a)  $L_1$ , (b)  $L_2$ , and (c)  $L_3$ .

the peaks at  $1661$  and  $1577\text{ cm}^{-1}$  strongly appeared and were assigned to the stretching vibration of  $\text{C}=\text{O}$  and  $\text{C}-\text{N}$  groups of polyamide. This spectrum indicates opening of the imide ring to the amide group. The adsorption region between  $2900$  and  $2850\text{ cm}^{-1}$  was attributed to the symmetric  $\text{C}-\text{H}$  stretching vibration of methylene groups of PEG-triazine. A wide peak appears between  $3200$  and  $3600\text{ cm}^{-1}$  and the peak at  $1417\text{ cm}^{-1}$  is assigned to the  $\text{O}-\text{H}$  and  $\text{C}-\text{O}$  stretching vibration of the hydroxyl group ( $-\text{C}-\text{O}-\text{H}$ ). These spectra indicate a successful modification.

#### Microscopic studies—SEM and AFM images

Effects of the PES/PI ratio on membrane morphology

To understand the influence of the PES/PI ratio on the membrane structure, the cross sections of the PES/PI blend membranes were obtained by SEM (Fig. 2). Among  $L_1$ ,  $L_2$ , and  $L_3$  membranes that have

the total concentration of 18 wt % (see Table I for the differences), the  $L_1$  membrane was prepared from PES with the lowest PI. This membrane [Fig. 2(a)] exhibits a typical asymmetric structure and fully developed macro-pores. The membrane structure comprises a dense thin top layer and a porous sub layer which is filled up by closed cells within the membrane matrix. Comparison of the images indicates that decreasing the PES/PI ratio decreases the skin layer thickness and changes the sub layer structure i.e., formation of finger-like macro-voids (large elongated pores). Figure 3 shows the order of the distance increase of the beginning of macrovoids to the membrane surface:  $L_1 > L_2 > L_3$  corresponds to the increasing order of the PES/PI ratio, i.e., decreasing the PES/PI ratio decreases the skin layer thickness. Longer macro-voids in the sublayer appear by decreasing the PES/PI ratio leading to higher porosity in the membrane structure. This results in higher permeability for the membrane.

The delay time for demixing is an important parameter for determining the membrane morphology.

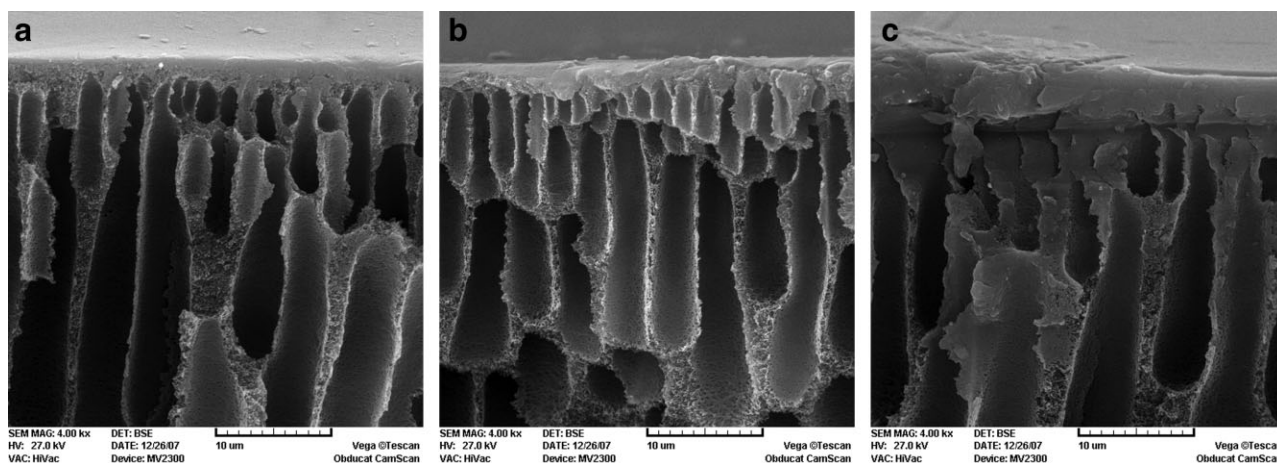


**Figure 4** Surface cross-sectional SEM morphology of: (a)  $L_6$ , (b)  $L_7$ , and (c)  $L_8$ .

**TABLE II**  
Chemical Surface Composition of Membranes (wt %)

Membrane	C	N	O	Cl	N/C
L <sub>EDA</sub>	93.81	0.98	5.21	0.00	1.04
L <sub>4</sub>	94.13	1.50	4.36	0.0107	1.59
L <sub>5</sub>	93.67	1.84	4.48	0.0085	1.96

Under rapid demixing conditions, membranes with a very thin top layer and a porous sublayer containing numerous macro-voids are expected. The top layer of these membranes often consists of nodular structures and possesses some degree of porosity. Under delayed demixing, membranes with a dense and thick top layer are anticipated.<sup>24</sup> In rapid demixing, the precipitation starts immediately after casting. This increases the polymer concentration in the vicinity of the interface region. The presence of the precipitated layer, creates an additional resistance to mass transfer between the coagulation bath and the sublayers of the solution. These conditions are convenient for nuclei growth and macro-pores formation. Under delayed demixing, membranes with a dense and thick top layer are anticipated.<sup>24</sup> In rapid demixing, the precipitation starts immediately after casting. This increases the polymer concentration in the vicinity of the interface region. The presence of the precipitated layer, creates an additional resistance to mass transfer between the coagulation bath and the sublayers of the solution. These conditions are convenient for nuclei growth and macro-pores formation.<sup>25</sup> Decreasing the PES/PI ratio affects the rates of nonsolvent inflow and solvent outflow.<sup>26</sup> The greater affinity of water and the PES/PI blend polymer compared with PES and water (major portion of the coagulation medium) results in rapid demixing. This leads to quick formation of a skin layer (creates an additional resistance to mass transfer) and results in a longer time for the entire exchange between the nonsolvent bath and the polymer casting film. Experimentally, the required time for the formation of the film made of PES/PI was much longer compared with the PES membrane. Increasing the exchange time between the solvent and nonsolvent results in more development of the growth and coalescence of the polymer-lean phase. Therefore, the larger finger-like pores are formed. As a rule of thumb, membranes with macro-voids usually have a very thin skin layer.

### Effect of chemical modification on membrane morphology

The SEM micrographs of cross sections of the membranes with and without modification are depicted in Figure 4. The modification influences the membrane morphology. In comparison with the unmodified membrane [Fig. 4(a)], the surfaces of the modified membranes [Fig. 4(b,c)] have been changed. A thicker skin layer is formed on the surface of membrane treated by DA [Fig. 4(c)]. The modified skin layer plays a key role in the separation property of the membranes and rejection capability. The elemental analysis data on the membrane surface using EDS are presented in Table II. These data support the evidence of surface modification. The element analysis for the L<sub>4</sub> membrane, modified by PEG-triazine, shows an increment in the atomic percentage of N and Cl compared with L<sub>EDA</sub> (the subscript refers to the membrane that is modified with EDA and this membrane was prepared to track the element analysis only). The modified membrane by DA (L<sub>5</sub>) indicates increasing in percentage of the N atom and decreasing in the Cl atom. This supports successful linking of the N atom from DA to the C atom from PEG-triazine on the membrane surface.

### Membrane pore size and roughness

Images of surfaces of membranes were obtained by AFM. Figure 5 shows images of the surfaces of L<sub>6</sub>, L<sub>7</sub>, and L<sub>8</sub> membranes. The dark areas represent membrane pores.<sup>27</sup> The surface roughness parameters of the membranes which are expressed in terms of the mean roughness ( $S_a$ ), the root mean square of the Z data ( $S_q$ ), the mean difference between the highest peaks and lowest valleys ( $S_z$ ) and the mean pore sizes of the membrane surface were calculated by SPM DME software (Table III). The sizes of the pores were measured from the height profile of two-

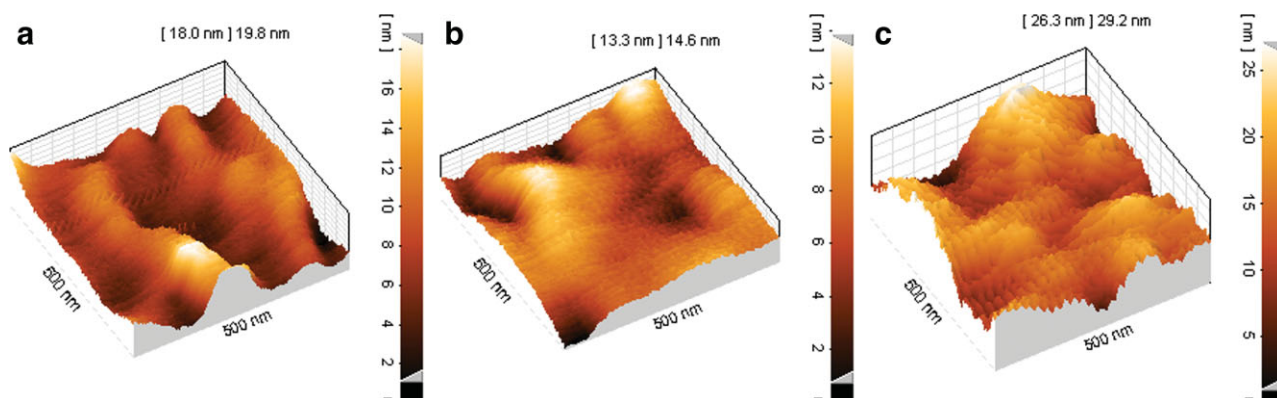


**Figure 5** AFM topographic images of: (a) L<sub>6</sub>, (b) L<sub>7</sub>, and (c) L<sub>8</sub>. [Color figure can be viewed in the online issue, which is available at [www.interscience.wiley.com](http://www.interscience.wiley.com).]



**TABLE III**  
The Mean Pore Size and the Roughness Parameters of Membrane Surfaces

Membrane	Mean pore size of surface (nm)	$S_z$	$S_a$	$S_q$
L <sub>6</sub>	100 (±45)	18.5	2.28	2.87
L <sub>7</sub>	55 (±30)	13.1	1.74	2.15
L <sub>8</sub>	35 (±21)	28.0	3.21	4.06

dimensional AFM images by using SPM software and the averages were reported.

The L<sub>6</sub> membrane possesses the darkest areas [Fig. 5(a)]. Modification of the membrane with EDA and PEG-triazine results in the formation of L<sub>7</sub> membrane [Fig. 5(b)]. The surface layer of the membrane had become slightly even and the dark area had become hidden. The modified membrane by EDA, PEG-triazine, and DA [L<sub>8</sub>-Fig. 5(c)] shows an increment in the convex area. This confirmed the formation of the surface layer. In general, Figure 6 indicates that modification changes the membrane surface's pore size and morphology. Moreover, the mean pore size of the membrane is decreased by modification. On the basis of the morphology alteration, the flux and rejection should be decreased and increased, respectively. Figure 5 supports this conclusion.

### Water contact angle

Hydrophilicities of obtained membranes were evaluated by measuring the static water contact angle. Table IV represents the water contact angles of L<sub>5</sub>, L<sub>6</sub>, L<sub>7</sub>, and L<sub>8</sub> membranes. Among Category 2, the contact angle of L<sub>6</sub> membrane was the highest value, 59.1°, whereas the modified membrane with DA (L<sub>8</sub>) showed the lowest contact angle, 51.4°. The PEG-triazine crosslinked membrane (L<sub>7</sub>) demonstrated the modest contact angle i.e., 56.2°. The presence of PEG-triazine on the membrane surface (L<sub>7</sub>) slightly enhances the hydrophilic property of the membrane. However, the modification of the L<sub>7</sub> membrane by DA (L<sub>8</sub>) remarkably increases the hydrophilicity of the membrane because of the appearance of -OH groups on the membrane surface (Fig. 1). Moreover,

**TABLE IV**  
Contact Angle of Obtained and Modified Membranes

Membrane	Contact angle (°)
Category 1	
L <sub>5</sub>	50.3 (±2.4)
Category 2	
L <sub>6</sub>	59.1 (±2.3)
L <sub>7</sub>	56.2 (±2.1)
L <sub>8</sub>	51.4 (±2.3)

**TABLE V**  
Flux and NaCl Rejection Capability of Membranes in Category 1

Membrane	Pure water flux (kg/m <sup>2</sup> h)	NaCl flux (kg/m <sup>2</sup> h)	Rejection (%)
L <sub>1</sub>	19.0 (±1.1)	16.7 (±1.0)	26.7 (±1.9)
L <sub>2</sub>	42.2 (±1.4)	38.0 (±1.2)	20.5 (±1.7)
L <sub>3</sub>	57.1 (±1.5)	55.5 (±1.5)	18.0 (±1.6)
L <sub>4</sub>	67.2 (±1.8)	64.0 (±1.6)	19.8 (±1.6)
L <sub>5</sub>	192.5 (±3.1)	187.2 (±2.2)	15.5 (±1.5)

the contact angle of the L<sub>5</sub> membrane, with similar modification to the L<sub>8</sub> membrane, was around 50.3°. However, the L<sub>5</sub> membrane with a lower ratio of PES/PI compared with that of the L<sub>8</sub> membrane, exhibited a higher flux.

### Membrane performance

The pure water flux, NaCl solution flux, and rejection behavior of membranes after 30 min are shown in Tables V and VI. The pure water fluxes of L<sub>1</sub>, L<sub>2</sub>, and L<sub>3</sub> membranes are 19.0, 42.2, and 57.1 kg/m<sup>2</sup> h, respectively. Flux increment is a function of the increasing PI. The flux of L<sub>4</sub> membrane (modified by 1 wt % DA) was 67.2 kg/m<sup>2</sup> h. However, the L<sub>5</sub> membrane (modified by 5 wt % DA) exhibited a very high flux i.e., 192.5 kg/m<sup>2</sup> h. The high content of DA in the L<sub>5</sub> membrane is responsible for increasing the hydrophilic property of the membrane leading to a high flux. Comparing L<sub>4</sub> and L<sub>5</sub> membranes indicates a remarkable flux development. This observation proves that the modification was successful in enhancing the hydrophilic property of the membrane. The L<sub>6</sub>, L<sub>7</sub>, and L<sub>8</sub> membranes with a high quantity (19 wt %) of polyethersulphone showed a low flux (around 3.85–4.07 kg/m<sup>2</sup> h—Table VI) and high rejection (between 73 to 92% for NaCl). This clearly represents the nanofiltration behavior for the membranes. The L<sub>1</sub> membrane with 16 wt % PES exhibits the highest rejection (25%) among the membranes in Category 1. This is not a property of the choice for a nanofiltration membrane. However, the second category membranes (L<sub>6</sub>, L<sub>7</sub>, and L<sub>8</sub>) with high salt rejection exhibit NF property.

**TABLE VI**  
Flux and NaCl Rejection Capability of Membranes in Category 2

Membrane	Pure water flux (kg/m <sup>2</sup> h)	NaCl flux (kg/m <sup>2</sup> h)	Rejection (%)
L <sub>6</sub>	3.85 (±0.07)	3.30 (±0.11)	73.7 (±2.0)
L <sub>7</sub>	4.30 (±0.12)	3.85 (±0.16)	81.4 (±2.5)
L <sub>8</sub>	4.07 (±0.10)	3.55 (±0.07)	92.3 (±2.3)

Considering the morphology and data for membranes in Category 1 (Figs. 2 and 5 and Table V) indicates that these membranes possess a high porosity and large surface pore size. They may be considered in the range of UF and MF membranes. The modification affects not only the membrane surface but also the membrane pores. In Category 2, because of the presence of thick and dense hydrophobic layers of PES, most probably, the modification occurs on the surface and a layer of the modifier is formed on the membrane surface leading to establishment of nanofiltration membranes. However, because of the presence of thick and dense hydrophobic layers of PES beneath the modified surface, there is no remarkable change in the flux. Conversely, the presence of the modifier layer on the surface leads to increasing the rejection. The images in Figure 4 and data in Table VI support this conclusion. The images show that the skin layer of the modified membrane is thicker compared with non-modified membranes leading to flux decline and rejection improvement.

### CONCLUSIONS

The blend membranes of polyethersulfone and polyimide were prepared in the presence of polyvinylpyrrolidone as pore former. The fabricated membranes were modified by EDA, PEG-triazine, and DA. The following results obtained from this study:

1. The successful modification was evidenced by SEM, AFM, FTIR-ATR, and contact angle measurements.
2. An increase in the pure water flux and a decrease in solute rejection are largely influenced by diminishing the PES/PI ratio. This is because of an increment in the membrane pore size and the porosity of the sub layer.
3. PI plays a role of a pore-forming additive that enhances the permeation property.
4. Hydrophilicity of PES/PI membranes is improved by modification.
5. Modification changes the property of the prepared MF/UF membranes into the NF membrane with low flux and high salt rejection.

We also thank Ms. Kheirollahi, Ms. Zarnegar and Mr. Moradian for their collaboration in this work.

### References

1. Chen, G.; Chai, X.; Yue, P. L.; Mi, Y. J. *Membr Sci* 1997, 127, 93.
2. Waypa, J. J.; Elimelech, M.; Hering, J. G. *J Am Water Works Assoc* 1997, 89, 102.
3. Nguyen, M. H.; Khan, M. M. A.; Kailasapathy, K.; Hourigan, J. A. *Austr J Dairy Tech* 1997, 52, 75.
4. Ericsson, B.; Hallberg, M.; Wachenfeldt, J. *Desalination* 1997, 108, 129.
5. Kharaka, Y. K.; Ambats, G.; Presser, T. S.; Davis, R. A. *Appl Geochem* 1996, 11, 797.
6. Huang, R.; Chen, G.; Sun, M.; Gao, C. *Sep Pur Technol* 2008, 58, 393.
7. Zhang, W.; He, G.; Gao, P.; Chen, G. *Sep Pur Technol* 2003, 30, 27.
8. Hellenbrand, R.; Mantzavinos, D.; Metcalfe, I. S.; Livingston, A. G. *Ind Eng Chem Res* 1997, 36, 5054.
9. Toyomoto, K.; Higuchi, A. In *Membrane Science and Technology*; Y. Osada, Y., Nakagawa, T., Eds.; Marcel Dekker: New York, 1992; p 289.
10. Kim, M.; Saito, K.; Furusaki, S.; Sugo, T.; Okamoto, J. *J Membr Sci* 1991, 56, 289.
11. Yamagishi, H.; Grivello, J. V.; Belfort, G. *J Membr Sci* 1995, 105, 237.
12. Steen, M. L.; Hymas, L.; Havey, E. D.; Capps, N. E.; Castner, D. G.; Fisher, E. R. *J Membr Sci* 2001, 188, 97.
13. Higuchi, A.; Koga, H.; Nakagawa, T. *J Appl Polym Sci* 1992, 46, 449.
14. Kim, K. J.; Fane, A. G.; Fell, C. J. D. *Desalination* 1988, 70, 229.
15. Khulbe, K. C.; Feng, C.; Matsuura, T.; Kapantaidakis, G. C.; Wessling, M.; Koops, G. H. *J Membr Sci* 2003, 226, 63.
16. Liang, K.; Grebowicz, J.; Valles, E.; Karasz, F. E.; MacKnight, W. J. *J Polym Sci, Part B: Pol Phys* 1992, 30, 465.
17. Ekiner, O. M. *Eur. Pat. Appl.* 0,648,812 A2 (1994).
18. Kapantaidakis, G. C.; Koops, G. H. *J Membr Sci* 2002, 204, 153.
19. Powell, C. E.; Duthie, X. J.; Kentish, S. E.; Qiao, G. G.; Stevens, G. W. *J Membr Sci* 2007, 291, 199.
20. Kim, Y. K.; Park, H. B.; Lee, Y. M. *J Membr Sci* 2005, 255, 265.
21. Namazi, H.; Adeli, M. *Polymer* 2005, 46, 10788.
22. Namazi, H.; Adeli, M. *J Polym Sci: Part A: Polym Chem* 2005, 43, 28.
23. Madaeni, S. S.; Mansourpanah, Y. *Desalination* 2004, 161, 13.
24. van de Witte, P.; Dijkstra, P. J.; van de Berg, J. W.; Feijen, J. *J Membr Sci* 1996, 117, 1.
25. Pereira, C. C.; Nobrega, R.; Borges, C. P. *J Membr Sci* 2001, 192, 11.
26. Young, T. H.; Chen, L. W. *J Membr Sci* 1991, 57, 69.
27. Dietz, P.; Hansma, P. K.; Inacker, O.; Lehmann, H.-D.; Herrmann, K.-H. *J Membr Sci* 1992, 65, 101.